Analysis of single-crystal Mossbauer data in low-symmetry ^{57}Fe centres

1992 J. Phys.: Condens. Matter 4 6993

(http://iopscience.iop.org/0953-8984/4/33/012)

J. Phys.: Condens. Matter 4 (1992) 6993–7008. Printed in the UK

Analysis of single-crystal Mössbauer data in low-symmetry ^{57}Fe centres

W C Tennant

New Zealand Institute for Industrial Research and Development*, PO Box 31-310, New Zealand

Received 14 April 1992

Abstract. The Mössbauer single-crystal experiment is discussed with particular reference to the low-symmetry resonant sites. It is demonstrated that ambiguities associated with multiple, symmetry-related resonant sites (that is, sites whose Laue class is lower than that of the host crystal) are resolvable provided the absorber recoilless fractions can be precisely measured. A general computer program, MOSREF, is described that enables simulation of single-crystal spectra and/or refinement of Mössbauer parameters for a ^{57}Fe centre in a site of any known symmetry in a host crystal of any known symmetry. The procedures are illustrated for a couple of ideal examples: a triclinic site in a monoclinic crystal and a monoclinic site in a trigonal crystal. Applications to recent experiments with the sheet micas biotite and muscovite are given.

1. Introduction

The Mössbauer technique has the potential to offer much valuable information from a study of the orientation dependence of such properties as intensity ratios of quadrupole doublets (leading to electric field gradient elucidation) and/or total intensities leading to absorber recoil-free fractions. The interpretation of such measurements may be simplified in the presence of internal or externally applied magnetic fields. Zory (1965) has calculated an analytical expression for the orientation dependence of the intensities of a quadrupole split doublet (no magnetic field interaction) applicable in the thin-crystal limit and indicated how these calculated intensities would be modified by absorber recoil-free fractions when more than one crystallographically equivalent site is present in the unit cell. Zimmermann (1975) later pointed out that in this latter case the different species contribute to the same quadrupole doublet and only a 'macroscopic' intensity tensor is observable. Gibb (1978) generalized this observation for all of the crystallographic point group symmetries and discussed the resolution of the ambiguities involved by the use of polarized radiation. Housley *et al* (1969) discussed the theory of coherence and polarization effects in Mössbauer absorption in single crystals and gave methods and restrictions for their correction in crystals of moderate thickness. Zimmermann (1983) later detailed these procedures using a simpler intensity tensor formalism.

The reasons that single-crystal Mössbauer measurements are not common are not difficult to find. One seldom finds a crystal which is at the same time 'thin', has only

* Previously DSIR Chemistry, New Zealand.

0953-8984/92/336993+16$04.50

one Mössbauer centre (i.e. has non-overlapping lines) and has sites of sufficiently high symmetry, in relation to host crystal symmetry, to yield a unique ('microscopic') intensity tensor.

2. Background considerations

At this laboratory we have (see McGavin *et al* 1980) in collaboration with others (see for example Mombourquette *et al* 1986) carried out extensive EPR algebraic and software development work aimed at obtaining extremely precise orientational properties of paramagnetic centres in single crystals. This generally involves many precise experimental measurements in one or more crystal planes followed by 'exact' numerical data fitting using matrix diagonalization of a theoretically correct spin Hamiltonian. The use of these techniques means that parameters associated with very small interactions can frequently be precisely determined and sometimes, otherwise indeterminate, ambiguities or degeneracies resolved.

In this paper a similar philosophy is applied to the Mössbauer single-crystal experiment. First a computer program (MOSREF) is outlined which computes by exact numerical diagonalization in arbitrary coordinates a theoretical Mössbauer spectrum for a Mössbauer centre in a site of any known symmetry in a crystal of any known symmetry. The program is also useable for simulating powder spectra from a set of single-crystal parameters by averaging the single-crystal spectra over a unit sphere. The calculation of absorber recoilless fractions is included. Then 'macroscopic' intensities can be computed for cases when there is more than one crystallographically equivalent site in the unit cell, e.g. when the Laue class (point group symmetry + a centre of inversion) of the site is lower than that of the host crystal (see table 1). In these cases the procedure of Weil *et al* (1973) is followed: calculations are carried out over the symmetry-related sites of the unit cell. The appropriate operations are the proper rotations of the 11 crystallographic proper rotation groups. Table 1, adapted from the generalized results for a second-rank tensor as presented by Rae (1972) and Weil *et al* (1973), shows the number of symmetry-related sites for each of the crystallographic point group symmetries (the table is similar to that presented for the Mössbauer case by Gibb (1978)). In the absence of a magnetic field, or for an arbitrarily oriented *internal* magnetic field, the spectra due to symmetry-related sites are summed into the same energy positions. As recognised by Zimmermann (1975) for quadrupole doublets, only a 'macroscopic' intensity tensor is then generally derivable. The magnetic hyperfine lines produced by an *external*, or combined internal–external, magnetic field will generally lead to distinct spectra for each symmetry-related site.

Herein we shall deal almost exclusively with the ambiguous ('low symmetry') spectra obtained for quadrupole split spectra obtained from multiple symmetry-related sites in the absence of a magnetic field. However the program described (MOSREF) includes both quadrupole and magnetic field interactions. Full details of the scope and operation of this program are to be published elsewhere (Tennant *et al* 1992b).

In the program MOSREF parameter refinement is effected by minimizing the squares of the differences between observed and calculated intensity ratios and, if recoil-free fractions are required, total intensities, again using matrix diagonalization and a suitable generalized minimization package. Here we use the package MINPACK developed by the Argonne National Laboratory (Morè *et al* 1980). If only a quadrupole interaction is present and the site and crystal Laue classes fulfil one of the

Table 1. Number of resonant sites for each point group symmetry.

	Triclinic	Monoclinic	Orthorhombic	Tetragonal		Trigonal		Hexagonal		Cubic	
					422				622		
		2	222	4	4mm		32	6	6mm		432
	1	m	mm2	$\bar{4}$	$\bar{4}$2m	3	3m	$\bar{6}$	$\bar{6}$m2	23	$\bar{4}$3m
Crystal[a]	$\bar{1}$	2/m	mmm	4/m	4/mmm	$\bar{3}$	$\bar{3}$m	6/m	6/mmm	m$\bar{3}$	m$\bar{3}$m
Site[b]	(C_i)	(C_{2h})	(D_{2h})	(C_{4h})	(D_{4h})	(C_{3i})	(D_{3d})	(C_{6h})	(D_{6h})	(T_h)	(O_h)
$\bar{1}$	1	2	4	4	8	3	6	6	12	12	24
2/m		1	2	2	4		3	3	6	6	12
mmm			1		2				3	3	6
4/m				1	1						3
4/mmm					1						3
$\bar{3}$						1	1	1	1	4	4
$\bar{3}$m							1		1		4
6/m								1	1		
6/mmm									1		
m$\bar{3}$										1	1
m$\bar{3}$m											1

[a] The final point group entry denotes the Laue crystal class which is also given, in parenthesis, in the Schönflies notation.

[b] The leftmost column gives the Laue class of the site.

conditions of table 1 for multiple resonant sites then only a 'macroscopic' intensity tensor is observable and in general the constituent 'microscopic' intensity tensors are indeterminate. Gibb (1978, 1974) has pointed out that this ambiguity is in principle resolvable by the use of polarized source radiation, though only a few practical cases have been reported (Gibb 1974).

In this work it is shown that simultaneous determination of the intensity and mean-squared displacement tensors can also in principle lead to a resolution of the ambiguity. The main problem here is precise enough determination of the mean-squared displacement tensor which is dependent upon measurement of anisotropy in the absorber recoil-free fractions (Goldanskii–Karyagan Effect). (This anisotropy is generally small though Grant *et al* (1969) by careful measurement obtained reliable data in their study of sodium nitroprusside.) For simultaneous intensity tensor and (MSD) tensor determination the minimization is also carried out across the measured total intensities appropriately corrected for background. It is assumed throughout this work that crystals are 'thin' or, when finite, that they are sufficiently thin for thickness and polarization corrections originally carried out by Grant *et al* (1969) and detailed by Zimmermann (1983) to be applicable. In the intensity tensor formalism of Zimmermann (1983) the thickness and polarization corrections require only a knowledge of the macroscopic intensity tensor which can always be obtained.

3. Theory

The appropriate Hamiltonian operator including nuclear quadrupole and, for completeness, magnetic field interactions can be written as

$$\mathcal{H} = -g_N\beta_N\left[(lB + l_1B_0)I_x + (mB + m_1B_0)I_y + (nB + n_1B_0)I_z\right] + \{eQ/[2I(2I-1)]\}\boldsymbol{I}\cdot\mathbf{V}\cdot\boldsymbol{I} \tag{1a}$$

$$\mathcal{H} = -g_N\beta_N\left[(A/2)I_+ + (A^*/2)I_- + (nB + n_1B_0)I_z\right] + [eQ/(2I(2I-1))]\left\{P\left[3I_z^2 - I(I+1)\right] + (b/4)I_+^2 + (b*/4)I_-^2 + c(I_zI_+ + I_+I_z)/2 + c*(I_zI_- + I_-I_z)/2\right\} \tag{1b}$$

where l, m, n and l_1, m_1, n_1 are elements of unit vectors along which the internal and external magnetic fields with magnitudes B and B_0 respectively are directed and

$$A = lB + l_1B_0 - \mathrm{i}(mB + m_1B_0) \qquad P = V_{zz} \qquad b = V_{xx} + V_{yy} - 2\mathrm{i}V_{xy}$$
$$c = V_{xz} - \mathrm{i}V_{yz}.$$

Here $A*$, $b*$ and $c*$ are the complex conjugates of A, b, c, respectively and V_{pq} $(p, q = x, y, z)$ are the elements of the symmetric traceless electric field gradient (EFG) tensor. The remaining symbols have their customary meanings. Also isotropic nuclear g-factors are assumed and we consider only the case of the ^{57}Fe nucleus with ground state, $I_g = \frac{1}{2}$, and excited state, $I_e = \frac{3}{2}$. The eigenvectors of (1*b*) are generally complex and must be obtained by numerical diagonalization.

Hereafter in this paper magnetic field interactions are neglected and equation (1*b*) is written in more concise form in terms of spherical tensor operators $\mathrm{T}_{l,m}(\mathbf{I})$. Following equation (10) of McGavin and Tennant (1985) tesseral combinations, $\mathcal{J}_{l,m}(\mathbf{I})$, of spherical tensor operators are taken when equation (1*b*) becomes

$$\mathcal{H} = [eQ/2I(2I-1)]\sum_{m=-2}^{2} a_{2,m}\mathcal{J}_{2,m}(\mathbf{I}) \tag{1c}$$

where the coefficients $a_{2,m}$ $(-2 \leqslant m \leqslant 2)$ are all real. In the Zimmermann (1975) intensity tensor formalism the EFG tensor, (V_{pq}) $(p, q = x, y, z)$, is replaced by an equivalent intensity tensor, (I_{pq}), proportional and diagonal in the same principal axis system. Then the invariant given by the sum of the squares of the coefficients $a_{2,m}$ has a constant value, 1/16 (Zimmermann 1975) and from equation (1*c*) can be obtained

$$\sum_{m=-2}^{2}(a_{2,m})^2 = I_{zz}^2 + (I_{xx} - I_{yy})^2/3 + 4\left(I_{xy}^2 + I_{xz}^2 + I_{yz}^2\right)/3$$
$$= -\mathrm{Tr}[\mathrm{Adj}(\mathbf{I})]/3 = 1/16. \tag{2}$$

We next need to know, in order to calculate transition probabilities, how the γ-radiation induces transitions amongst the complex eigenstates of equation (1*c*). Here

we essentially follow Housley *et al* (1969). Magnetic dipole radiation from a ^{57}Co source can be described by the basis kets, in the $|JM\rangle$ notation,

$$|1\ 1\rangle = -(1/\sqrt{2})(e_X + ie_Y)e^{i\omega t} \tag{3a}$$

$$|1\ -1\rangle = (1/\sqrt{2})(e_X - ie_Y)e^{i\omega t} \tag{3b}$$

$$|1\ 0\rangle = e_X e^{i\omega t}. \tag{3c}$$

Equations (3*a*), (3*b*) refer respectively to the right- and left-hand circular components of the magnetic dipole radiation. It is required to refer this radiation to the x, y, z laboratory Cartesian frame. The new coordinates are specified by performing a rotation ϕ about the Z-axis followed by a rotation θ about the resulting Y-axis where θ, ϕ are the polar and aximuthal angles describing the direction of propagation of the γ-beam with respect to the laboratory axes, that is

$$R_{Y'}(\theta)R_Z(\phi)\begin{vmatrix} e_X \\ e_Y \\ e_Z \end{vmatrix} = \begin{vmatrix} \cos\theta & 0 & -\sin\theta \\ 0 & 1 & 0 \\ \sin\theta & 0 & \cos\theta \end{vmatrix}\begin{vmatrix} \cos\phi & \sin\phi & 0 \\ -\sin\phi & \cos\phi & 0 \\ 0 & 0 & 1 \end{vmatrix}\begin{vmatrix} e_X \\ e_Y \\ e_Z \end{vmatrix} \tag{4}$$

or

$$\begin{vmatrix} e_x \\ e_y \\ e_z \end{vmatrix} = \begin{vmatrix} \cos\theta\cos\phi & \cos\theta\sin\phi & -\sin\theta \\ -\sin\phi & \cos\phi & 0 \\ \sin\theta\cos\phi & \sin\theta\sin\phi & \cos\theta \end{vmatrix}\begin{vmatrix} (-|1\ 1\rangle + |1\ -1\rangle)/\sqrt{2} \\ i(|1\ 1\rangle + |1\ -1\rangle)/\sqrt{2} \\ |1\ 0\rangle \end{vmatrix}. \tag{5}$$

Here e_x, e_y, e_z and e_X, e_Y, e_Z are Cartesian unit vectors in the new (laboratory, x, y, z) and old (radiation, X, Y, Z) frames respectively. In the literature (see for example Housley *et al* 1969) an alternative spherical unit vector nomenclature ϕ, θ, r is often used in place of e_x, e_Y, e_z. For simplicity in equations (4) and (5), and hereafter, the exponential factors of equations (3) have been omitted. Then in the new basis the 'transformed' radiation is

$$|1\ 1\rangle' = -(e_x + ie_y)/\sqrt{2}$$

$$= \tfrac{1}{2}[(1+\cos\theta)e^{i\phi}|1\ 1\rangle + (1-\cos\theta)e^{i\phi}|1\ -1\rangle + \sqrt{2}\sin\theta|1\ 0\rangle] \tag{6}$$

$$|1\ -1\rangle' = (e_x - ie_y)/\sqrt{2}$$

$$= \tfrac{1}{2}[(1-\cos\theta)e^{i\phi}|1\ 1\rangle + (1+\cos\theta)e^{i\phi}|1\ -1\rangle - \sqrt{2}\sin\theta|1\ 0\rangle]. \tag{7}$$

From equations (6) and (7) the intensities between the basis ground and excited state kets, $|E_g\rangle$ and $|E_e\rangle$ respectively, are calculated using the usual rules of vector coupling and the appropriate Clebsch–Gordan coefficients. These matrix elements are set out as 2×4 arrays $\mathbf{R}_R$ and $\mathbf{R}_L$ in table 2 where the subscripts R and L refer to right- and left-hand circular polarization respectively. $\mathbf{R}_R$ and $\mathbf{R}_L$ are intensity operator matrices and in the computer calculations the intensities of individual magnetic hyperfine transitions are obtained as the elements of the 2×4 matrix $\mathbf{P}$ where

$$\mathbf{P} = |\mathbf{E}_g\mathbf{R}_R\mathbf{E}_e|^2 + |\mathbf{E}_g\mathbf{R}_L\mathbf{E}_e|^2. \tag{8}$$

Table 2. Intensity operator matrices $\mathbf{R}_R$ and $\mathbf{R}_L$ describing coupling of ground $I_g = \frac{1}{2}$ and excited $I_e = \frac{3}{2}$ kets by $|1\ -1\rangle'$ and $|1\ -1\rangle'$ radiation (equations (6), (7)).

(a) $|1\ 1\rangle'$ radiation (matrix $\mathbf{R}_R$).

	$\|3e/2\ -3/2\rangle$	$\|3e/2\ -1/2\rangle$	$\|3e/2\ 1/2\rangle$	$\|3e/2\ 3/2\rangle$
$\langle ½g\ ½\|$	0	$2/3(1-\cos\theta)e^{i\phi}$	$\sin\theta/\sqrt{3}$	$½(1+\cos\theta)e^{-i\phi}$
$\langle ½g\ -½\|$	$½(1-\cos\theta)e^{i\phi}$	$\sin\theta/\sqrt{3}$	$2/3(1+\cos\theta)e^{-i\phi}$	0

(b) $|1\ -1\rangle'$ radiation (matrix $\mathbf{R}_L$).

	$\|3e/2\ -3/2\rangle$	$\|3e/2\ -1/2\rangle$	$\|3e/2\ 1/2\rangle$	$\|3e/2\ 3/2\rangle$
$\langle ½g\ ½\|$	0	$2/3(1+\cos\theta)e^{i\phi}$	$-\sin\theta/\sqrt{3}$	$½(1-\cos\theta)e^{-i\phi}$
$\langle ½g\ -½\|$	$½(1+\cos\theta)e^{i\phi}$	$-\sin\theta/\sqrt{3}$	$2/3(1-\cos\theta)e^{-i\phi}$	0

Here $\mathbf{E}_g$ and $\mathbf{E}_e$ are the 2×2 and 4×4 eigenvector matrices of the ground and excited states respectively. It is clear that all computations must be in complex arithmetic.

In general the total intensities will be modified by absorber recoil-free fractions having values less than unity. Each calculated intensity is modified, as described by Zory (1965) and Grant *et al* (1969), by a factor $f_i = \exp[-k^2\langle r^2\rangle_i]$. Here $k^2 = 4\pi^2/\lambda^2$ where λ is the wavelength of the radiation and f_i and $\langle r^2\rangle_i$ are the values of the recoil-free fraction and mean-squared displacement respectively for the ith site; k^2 for ^{57}Fe is (Grant *et al* 1969) 5.33×10^{17} cm^{-2}. In the present work anisotropy in the recoil-free fractions is incorporated optionally in the intensity calculations. Whenever there is more than one crystallographically equivalent site in the unit cell one needs to input the rotation matrices of the symmetry-related sites for the appropriate Laue crystal class. These matrices are obtainable from table 2 of Weil *et al* (1973). In the program such calculations are included for up to four symmetry-related sites so that all but a few cases can be handled in monoclinic, orthorhombic, tetragonal, trigonal and hexagonal crystals (refer to table 1).

4. Applications

The program MOSREF, as outlined, can be used in two ways as follows.

4.1. Simulation

Calculation of intensity ratios and total intensities. Two cases are considered:

Case 1. The Laue class of the site and the Laue class of the crystal are the same, e.g. point group symmetry of site 2, m, or $2/m$ in a monoclinic crystal with point group symmetry 2, m, or $2/m$. Only a single species is observed in all crystal orientations (see table 1 and refer to Rae (1972), Weil *et al* (1973) and Gibb (1978) for generalization). The user inputs the EFG (i.e. intensity) tensor (and magnitude and direction cosines of the internal/external magnetic field vectors, if present) and the polar and azimuthal angles θ and ϕ of the γ-radiation direction with respect to the laboratory axes x, y, z for which intensity calculations are required (refer to figure 1). The mean-squared displacement, $\langle$MSD$\rangle$, tensor elements may also be input (as dimensionless quantities $k^2\langle r^2\rangle$ where $\langle r^2\rangle$ is the value of the mean-squared displacement in units 10^{-18} cm^2 and k^2 for ^{57}Fe is 0.533×10^{18} cm^{-2}). This affects the total intensity of a quadrupole doublet but not the relative intensities of its two component peaks.

Case 2. The Laue class of the site is lower than the Laue class of the host crystal. For example point group symmetry 1 (Laue class $\bar{1}$) in a monoclinic crystal or point group symmetry 2 (Laue class $2/m$) in a trigonal crystal (we shall use these examples later). Input data is as for case 1. Generally more than one species is present (table 1) and each is observable as a distinct spectrum in the presence of an external magnetic field. If only a nuclear electric quadrupole interaction is present then, as discussed above, only a single spectrum is observed which is the sum of two or more 'microscopic' spectra. We discuss the ambiguities involved, and their resolution, in the discussion on parameter refinement below.

In both cases above, and in general, the symmetry requirements of the EFG and $\langle$MSD$\rangle$ tensors as second rank crystal physical properties needs to be recognized. For example in the trigonal example in case 2 both tensors must have one principal axis directed along the crystal twofold axis (see Nye (1957) for generalization).

Once single crystal simulation has been achieved it is a simple matter to simulate the intensity pattern of a powder by averaging all single-crystal orientations over a unit sphere. This option is included in the program MOSREF.

4.2. Parameter refinement

Here the following basic requirements are assumed. There must be sufficient data to yield a unique solution; this requires more data points than parameters to be refined, the data being collected from crystal orientations in two or more distinct crystal planes in order to allow the determination of the EFG and $\langle$MSD$\rangle$ tensor elements. The number of independent tensor elements to be determined depends on the site symmetry. For a single Mössbauer centre, the ('microscopic') EFG (or intensity) tensor is governed by both the zero-trace invariance condition and by the invariance condition, equation(2). Hence it is only necessary generally to determine four independent intensity tensor elements. There are no such constraints on the symmetric $\langle$MSD$\rangle$ tensor and in general six independent tensor elements must be determined. There is no general requirement for the principal axes of the two tensors to be coincident. It is assumed also that either the thin-crystal limit is applicable or that data has been corrected for thickness and polarization effects as outlined by Grant *et al* (1969) and detailed by Zimmermann (1983). The crystal 'thickness' must

be sufficiently small for the corrections to be valid. Our own experience with a rather thick biotite crystal (Aldridge *et al* 1991) would indicate an upper limit of around 20 mg cm^{-2} total iron as appropriate. As noted earlier, thickness and polarization corrections in the intensity tensor formalism of Zimmermann (1975) require only a knowledge of the macroscopic intensity tensor. The process is iterative; new thickness and polarization corrections need to be calculated from the updated intensity tensor as refinement proceeds towards convergence.

Again two cases are considered, restricting attention to a quadrupole interaction only.

Case 1. There is no site ambiguity. The user supplies as input measured (thickness and polarization corrected) intensity ratios and direction cosines giving the orientations of the γ-radiation in the chosen laboratory frame (fixed in the crystal). If the mean-squared displacement tensor is to be determined, the user also supplies measured total intensities obtained, after background correction, as the sums of dimensionless areas of pairs of quadrupole lines. Trial estimates of the EFG and ⟨MSD⟩ tensor elements are also supplied. Experience shows that these are not critical for successful convergence: a reasonable first estimate for the EFG tensor is usually possible (for example the macroscopic intensity tensor is usually obtainable from a straightforward analysis of intensity ratio data) and the 3×3 identity matrix is usually sufficient as a first estimate for the ⟨MSD⟩ tensor. Output consists of the best-fit EFG and ⟨MSD⟩ tensors and their principal values and directions, obtained by numerical diagonalization, referred to the laboratory frame. A listing of calculated and observed intensities and calculated recoil-free fractions in each crystal orientation is also given.

Case 2. An ambiguous case (Laue class of site is lower than that of crystal). Input is as above except that total intensities *must* be input unless only the macroscopic EFG tensor is required. The user must also input the number of symmetry-related sites in the unit cell and the proper rotation matrices relating the sites. Output is as above; EFG and ⟨MSD⟩ tensors are given for each of the symmetry-related sites.

Resolution of an ambiguous case is dependent upon being able to accurately measure the anisotropy in the sample recoil-free fraction and there are obvious advantages in carrying out measurements in a sufficient number of crystal orientations to considerably over-determine the ⟨MSD⟩ tensor. For example in a study of several biotite crystals (Tennant *et al* 1992a) data was collected in 12 orientations in one plane and in 6 other orientations in different crystal planes, a total of 18 crystal orientations (see further comment later).

5. Some examples

Here a couple of examples of parameter refinement are presented based on idealized data to illustrate the use of the program MOSREF. Again attention is restricted to examples where only a quadrupole interaction is present. Refer to the coordinate system defined by figure 1. The crystal is assumed to be a thin slab containing the y- and z-axes of the laboratory frame; x is normal to the slab. $\hat{\gamma}$ is a unit vector along which the γ-radiation is directed and θ and ϕ are the polar and azimuthal angles defining the γ-direction in the x, y, z system.

Example 1. A single site of triclinic symmetry in a monoclinic crystal. The Laue class of the site and crystal are $\bar{1}$ and $2/m$ respectively and there are (table 1) two

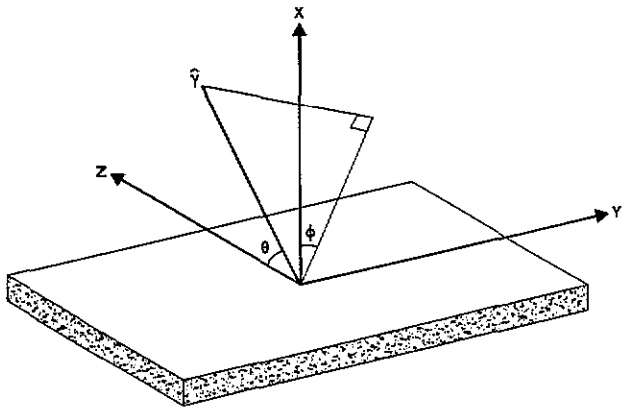

Figure 1. The laboratory axis system used for a thin crystal plate; $\hat{\gamma}$ is an arbitrary vector along which the γ-beam is directed.

crystallographically equivalent sites related by rotation of 180° about the b-axis. In figure 1 we choose b along the z-axis and assume the following intensity (EFG) and ⟨MSD⟩ tensors:

Intensity tensor:

$$I_{\hat{x}\hat{x}} = 0.037\,427 \qquad \theta_c = 30° \qquad \phi_c = 30°$$
$$I_{\hat{y}\hat{y}} = 0.195\,359 \qquad \theta_c = 120° \qquad \phi_c = 30°$$
$$I_{\hat{z}\hat{z}} = 0.232\,776 \qquad \theta_c = 90° \qquad \phi_c = 120°$$

$$\mathbf{S} = \begin{vmatrix} 0.433\,013 & 0.750\,000 & -0.500\,000 \\ 0.250\,000 & 0.433\,013 & 0.866\,025 \\ 0.866\,025 & -0.500\,000 & 0.000\,000 \end{vmatrix}$$

⟨MSD⟩ tensor:

$$\langle\hat{x}\hat{x}\rangle = 0.679\,858 \qquad \theta_c = 90° \qquad \phi_c = 0°$$
$$\langle\hat{y}\hat{y}\rangle = 0.772\,177 \qquad \theta_c = 95° \qquad \phi_c = 90°$$
$$\langle\hat{z}\hat{z}\rangle = 0.822\,213 \qquad \theta_c = 5° \qquad \phi_c = 90°$$

$$\mathbf{S}' = \begin{vmatrix} 1.000\,000 & 0.000\,000 & 0.000\,000 \\ 0.000\,000 & 0.996\,195 & 0.087\,156 \\ 0.000\,000 & -0.087\,156 & 0.996\,195 \end{vmatrix}$$

where θ_c and ϕ_c are the polar and azimuthal angles of the principal directions and $\mathbf{S}$ and $\mathbf{S}'$ are the corresponding (column) eigenvector matrices. The magnitudes of the principal values assumed here are identical with those found in a recent study of Fe^{2+} centes in 1M biotites (Tennant *et al* 1992a). The usual convention of labelling the principal values of the intensity tensor with the largest magnitude as $I_{\hat{z}\hat{z}}$ has been followed. There is no such convention for the ⟨MSD⟩ tensor but again the diagonal element with the largest (positive) value has been labelled $\langle\hat{z}\hat{z}\rangle$ throughout. Note that the principal values in the intensity tensor conform to the two invariants, zero

are given in terms of the product $k^2\langle r^2\rangle$ where k^2 for ^{57}Fe is 5.33×10^{17} cm^{-2}. The relation $f' = \exp[-k^2\langle r^2\rangle]$ then gives both the recoilless fraction f' and the mean-squared displacement $\langle r^2\rangle$. Numerical values of both of these quantities are output by program MOSREF. The $\langle zz\rangle$ principal direction has been deliberately chosen to be close to the b-axis; when the two coincide the problem is indeterminate since both sites have identical $\langle$MSD$\rangle$ tensors. From the above data the 'experimental' tensors are obtained (with $p, q = x, y, z$) as

$$(I_{pq}) = \begin{vmatrix} 0.058\,711 & 0.168\,290 & -0.059\,228 \\ 0.168,290 & -0.135\,614 & -0.034\,196 \\ -0.059\,228 & -0.034\,196 & 0.076\,903 \end{vmatrix}$$

$$(\langle pq\rangle) = \begin{vmatrix} 0.679\,858 & 0.000\,000 & 0.000\,000 \\ 0.000\,000 & 0.772\,558 & 0.004\,344 \\ 0.000\,000 & 0.004\,344 & 0.821\,833 \end{vmatrix}.$$

Using these matrices as input, 'experimental' (thin-crystal limit) intensity ratios and total intensities were simulated in the following planes (refer to figure 1): $\theta = 90°$, $\phi = 0°$, $\pm 30°$, $\pm 55°$; $\theta = 75°$, $\phi = 0°$, $\pm 15°$, $\pm 30°$; $\theta = 60°$, $\phi = 0°$, $\pm 15°$, $\pm 30°$; $\theta = 45°$, $\phi = 0°$, $\pm 15°$, $\pm 30°$. These planes were chosen as being practically realizable for a reasonably large thin-crystal plate.

For refinement the computed intensities were input together with crude estimates of intensity and $\langle$MSD$\rangle$ tensors. It turns out that neither are critical to eventual convergence but reasonable estimates speed the process up. In this example the macroscopic intensity tensor is readily obtainable by a straightforward least squares fitting of any one plane of data to an expression of the form $I = A + B \cos 2\phi + C \sin 2\phi$. Only the xz and yz components of the intensity tensor are then unknown, but from equation (2) $I_{xz}^2 + I_{yz}^2$ is known. Most conveniently we proceed as follows. Step 1: input the macroscopic intensity tensor with $I_{xz} = I_{yz} = \pm\frac{1}{2}(I_{xz}^2 + I_{yz}^2)^{1/2}$ (or indeed $I_{xz} = I_{yz} = 0$, although in this case equation (2) is not satisfied) and unit identity matrix for $\langle$MSD$\rangle$; refine only the $\langle$MSD$\rangle$ tensor (there are however small consequent changes to the intensity tensor due to operation of the condition set by equation (2)). Step 2: input the macroscopic intensity tensor as in step 1 and the refined $\langle$MSD$\rangle$ tensor; refine simultaneously intensity and $\langle$MSD$\rangle$ tensors. The results of the refinements are summarized in tables 3 and 4; only the lower triangles of symmetric matrices are given.

Example 2. A site of symmetry 2 (C_2) in a trigonal crystal of point group symmetry 32 (D_3), Laue classes $2/m$ and $\bar{3}m$ respectively, was chosen. There are (table 1) three symmetry-related sites and the proper rotation matrices relating sites 2 and 3 to site 1 are (Weil *et al* 1973):

$$\mathbf{R}_{\pm} = \begin{vmatrix} -1/2 & 0 & \mp\sqrt{3}/2 \\ 0 & 1 & 0 \\ \pm\sqrt{3}/2 & 0 & -1/2 \end{vmatrix}. \tag{9}$$

The choice of laboratory axes (fixed in the crystal) are here: twofold crystal axis along z (as in example 1) and threefold (or, threefold screw) crystal axis along y; the principal EFG and $\langle$MSD$\rangle$ tensor values are as for example 1 and principal directions as follows (all data here was taken from an actual experiment: a monoclinic site in 1M biotite (Tennant *et al* 1992a)):

Table 3. Refinement details for ideal monoclinic example (example 1).

Step 1

Input matrices (site 1)							
(I_{pq}) =	0.058			(<pq>) =	1.0		
	0.168	-0.136			0.0	1.0	
	0.0	0.0	0.078		0.0	0.0	1.0
RMSD[a] = 1.332693							

Refined matrices (site 1)							
(I_{pq}) =	0.061			(<pq>) =	0.679858		
	0.177	-0.143			0.000000	0.772558	
	0.000	0.000	0.082		0.000459	0.000364	0.821826
RMSD = 0.004012; No. of iterations = 12							

Step 2

Input matrices (site 1)							
(I_{pq}) =	0.058			(<pq>) =	0.679858		
	0.168	-0.136			0.000000	0.772558	
	0.0	0.0	0.078		0.000459	0.000364	0.821826
RMSD = 0.043962							

Refined matrices (site 1)							
(I_{pq}) =	0.058711			(<pq>) =	0.679858		
	0.168290	-0.135614			0.000000	0.772558	
	-0.059234	-0.034187	0.076903		-0.000001	0.004355	0.821833
RMSD = 0.000002; No. of iterations = 27							

[a]RMSD = Root mean squared deviation

Intensity tensor:

$$I_{\hat{x}\hat{x}} = 0.037\,417 \qquad \theta_c = 0°$$

$$I_{\hat{y}\hat{y}} = 0.195\,359 \qquad \theta_c = 90° \qquad \phi_c = 67°27.2'$$

$$I_{\hat{z}\hat{z}} = 0.232\,776 \qquad \theta_c = 90° \qquad \phi_c = -22°32.8'$$

$$\mathbf{S} = \begin{vmatrix} 0.000\,000 & 0.383\,432 & 0.923\,569 \\ 0.000\,000 & 0.923\,569 & -0.383\,432 \\ 1.000\,000 & 0.000\,000 & 0.000\,000 \end{vmatrix}$$

$\langle$MSD$\rangle$ tensor:

$$\langle \hat{x}\hat{x} \rangle = 0.679\,858 \qquad \theta_c = 90° \qquad \phi_c = 107°10.8'$$

$$\langle \hat{y}\hat{y} \rangle = 0.772\,177 \qquad \theta_c = 0°$$

$$\langle \hat{z}\hat{z} \rangle = 0.822\,213 \qquad \theta_c = 90° \qquad \phi_c = 17°10.8'$$

$$\mathbf{S}' = \begin{vmatrix} -0.295\,375 & 0.000\,000 & 0.955\,382 \\ 0.955\,382 & 0.000\,000 & 0.295\,375 \\ 0.000\,000 & 1.000\,000 & 0.000\,000 \end{vmatrix}.$$

Table 4. Calculated and 'observed' EFG and ⟨MSD⟩ principal values and directions[a] for site 1 (example 1).

	Calculated			Observed		
	Principal Values	Principal Directions		Principal Values	Principal Directions	
p	I_{pp}	θ	ϕ	I_{pp}	θ	ϕ
z	-0.232776	90°0.1′	120°0.0′	-0.232776	90°	120°
x	0.037417	30°0.0′	30°0.2′	0.037417	30°	30°
y	0.195359	120°0.0′	30°0.1′	0.195359	120°	30°
	$<\hat{p}\hat{p}>$	θ	ϕ	$<\hat{p}\hat{p}>$	θ	ϕ
x	0.679858	90°0.0′	0°0.0′	0.679858	90°	0°
y	0.772176	95°0.7′	90°0.0′	0.772177	95°	90°
z	0.822215	5°0.7′	90°0.4′	0.822213	5°	90°

[a] Site 2 principal directions are $\theta, \phi + 180°$.

Proceeding as for example 1 ;the 'experimental' tensors are:

$$(I_{pq}) = \begin{vmatrix} -0.169\,832 & 0.151\,614 & 0.000\,000 \\ 0.151\,614 & 0.132\,415 & 0.000\,000 \\ 0.000\,000 & 0.000\,000 & 0.037\,417 \end{vmatrix}$$

$$(\langle pq \rangle) = \begin{vmatrix} 0.809\,750 & 0.040\,313 & 0.000\,000 \\ 0.040\,313 & 0.691\,821 & 0.000\,000 \\ 0.000\,000 & 0.000\,000 & 0.772\,177 \end{vmatrix}.$$

As before 'experimental' intensities were simulated in 20 crystal orientations chosen in four distinct planes. In this instance a one step procedure from an initial crude set of intensity tensor and ⟨MSD⟩ tensor values was followed. The results of refinement are summarized in tables 5 and 6.

6. Discussion

It is clear from the two examples illustrated that rapid convergence to 'true' values from a reasonable, but not critical, set of starting values is achieved. The principal directions in terms of polar and azimuthal angles are 'correct' to better than one minute of arc which is about an order of magnitude better than is usual for practical crystal alignment in Mössbauer experiments.

What is the situation for real-world crystals and experiments Some limitations were set out in the introduction. In more detail the following requirements need to be met for practical resolution of single-crystal Mössbauer experiments. (We refer only to cases when the magnetic field interaction is absent and only to ^{57}Fe).

Table 5. Refinement details for ideal trigonal example (example 2).

Input matrices (site 1)								
(I_{pq}) =	-0.15			(<pq>) =	1.0		
	0.1	0.1			0.0	1.0	
	0.0	0.0	0.05		0.0	0.0	1.0
RMSD = 1.087596							

Refined matrices (site 1)								
(I_{pq}) =	-0.169813			(<pq>) =	0.809744		
	0.151627	0.132414			0.040309	0.691821	
	0.0	0.0	0.037399		0.0	0.0	0.772183
RMSD = 0.000002; No. of iterations = 7								

Table 6. Calculated and 'observed' EFG and ⟨MSD⟩ tensor principal values and principal directions[a] for site 1 (example 2).

	Calculated			Observed		
	Principal Values	Principal Directions		Principal Values	Principal Directions	
p	$I_{\hat{p}\hat{p}}$	θ	ϕ	$I_{\hat{p}\hat{p}}$	θ	ϕ
z	-0.232770	90°	-22°32.9′	-0.232776	90°	-22°32.8′
x	0.037399	0°	-	0.037417	0°	-
y	0.195371	90°	67°27.1′	0.195359	90°	67°27.2′
	$\langle\hat{p}\hat{p}\rangle$	θ	ϕ	$\langle\hat{p}\hat{p}\rangle$	θ	ϕ
x	0.679359	90°	107°10.7′	0.679357	90°	107°10.8′
y	0.772183	0°	-	0.772176	0°	-
z	0.822206	90°	17°10.7′	0.822213	90°	17°10.8′

[a] Site 2 and site 3 principal directions are obtained from equations $\mathbf{V}_{2,3} = \mathbf{R}_{\pm}.\mathbf{V}_1$ where $\mathbf{V}_a$ (a = 1, 2, 3) are the principal direction eigenvectors for sites 1, 2 and 3 respectively and $\mathbf{R}_{\pm}$ are the rotation matrices of equations (9).

(i) Crystals are required which are physically thin and also 'thin' in terms of the number of resonant nuclei per unit of crystal area in order that corrections to the 'thin-crystal limit' (Grant *et al* 1969) are valid. Ideally a thin plate which can be rotated in the γ-beam is required. Alternatively, as presented by Grant *et al* (1969) several plates cut in different crystal planes and each mounted normal to the γ-beam, can be used. If total quadrupole intensities (areas) are to be measured (for ⟨MSD⟩ tensor determination) then it must be arranged, by beam collimation and crystal shielding, that all γ-radiation reaching the detector has passed through the crystal in

order to validate the corrections made for background arising from non-Mössbauer gamma quanta.

(ii) Strictly polarization and coherence effects in the Mössbauer effect in single crystals are only defined for single isolated resonant centres (Blume and Kistner 1968, Housley *et al* 1969). In most real-world crystals (e.g. minerals) there are multiple sites present and commonly iron in more than one oxidation state leading to overlapping lines. Thickness and polarization corrections as outlined by Grant *et al* (1969) are then strictly not valid.

(iii) In order for the methods of this paper to be applicable to ambiguous cases, as exemplified by example 2 of the previous section, it is necessary to be able to measure, with reasonable precision, anisotropy in absorber recoilless fractions. There are few reported such measurements in the literature for ^{57}Fe and the effect is generally supposed to be vanishingly small in this instance; however see Clark *et al* (1967) and Grant *et al* (1969). The latter of these papers reports mean-squared displacements for Fe in sodium nitroprusside ranging from 1.665 to 1.905 $\times$ 10^{18} cm^{-2}, i.e. a 15% anisotropy, which is about the same as used in the ideal examples of the last section. A more extreme example, recently reported, is that of the superconducting phase $YBa_2(Cu_{1-x}Fe_x)_4O_8$ where recoilless fractions measured parallel and perpendicular to the magnetic axis were found to vary by a factor of about two (Boolchand *et al* 1992).

At this laboratory we have recently been carrying out Mössbauer measurements on single crystals of the sheet micas biotite and muscovite. Figure 2 shows measured dimensionless peak areas for Fe^{2+} in the *cis*-site of a 1M biotite and a $2M_1$ muscovite. Also shown are the recoilless fractions which show considerable anisotropy—certainly sufficient for the methods of this paper to be applicable. Full details of this work are to be published elsewhere (Tennant *et al* 1992a, Tennant *et al*, to be published).

There will always of course be accidental degeneracies or coincidences of EFG and ⟨MSD⟩ tensor principal directions which will make some of the methods presented here invalid. Such a case was alluded to in the first ideal example: if a principal axis of the ⟨MSD⟩ tensor for a $\bar{1}$ site in a monoclinic crystal were to lie along the twofold axis, then the problem is indeterminate; only a 'macroscopic' intensity tensor is obtainable. There is no reason on symmetry grounds for this to be so although we note that Grant *et al* (1969) have stated that ⟨MSD⟩ principal directions should be strongly influenced by long-wavelength vibrations in the crystal and may well be related to lattice symmetry rather than local symmetry. There could consequently be instances where the ⟨MSD⟩ principal directions would lie along crystallographic axes.

Experience in EPR single crystal measurements indicates that considerable advantage is to be gained by making measurements in a sufficiently large number of crystal orientations to considerably over-determine tensor quantities of small magnitude. This is undoubtedly the case for the ⟨MSD⟩ tensor in Mössbauer experiments but this needs to be balanced against the tedious nature of the experiment (at this laboratory we typically collect about 5 $\times$ 10^6 background counts per crystal orientation).

7. Conclusions

The feasibility of Mössbauer parameter refinement from single-crystal data for all resonant site symmetries in crystals of any symmetry has been demonstrated. To resolve the ambiguities associated with low-symmetry sites it is necessary to be able

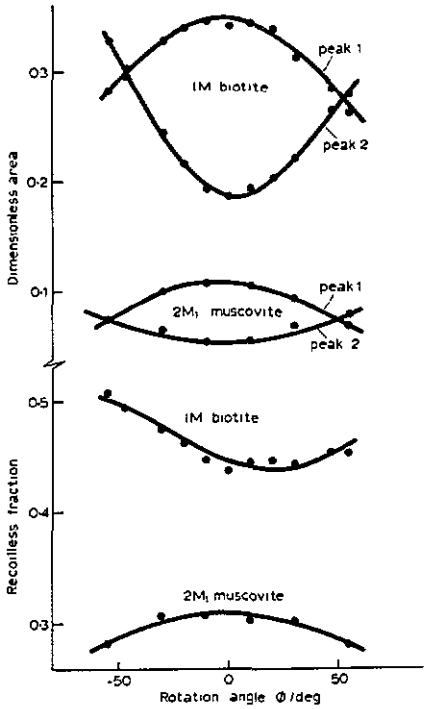

Figure 2. Angular dependence of dimensionless areas and recoilless fractions for Fe^{2+} in the *cis*-octahedral sites of a 1M biotite and a $2M_1$ muscovite; the plane of observation is perpendicular to the monoclinic twofold axis in both cases.

to measure single-crystal (anisotropic) absorber recoilless fractions with considerable precision. This requires many measurements in two or more distinct crystal planes in order to considerably over-determine the mean-squared displacement tensor. The advantage of the methods outlined in this paper is that the determination of microscopic tensors is possible for all site and crystal symmetries from data collected in a conventional Mössbauer experiment; polarized source radiation is not, for example, required. The disadvantages are the difficulties in obtaining a meaningful ⟨MSD⟩ tensor, and the (consequent) tedious nature of the experiment.

Acknowledgments

The author is grateful to Dr D G McGavin for his critical comments on this manuscript and for his contribution in writing the error analysis portions of the program MOSREF described in the text.

Appendix

The following is a list of options available in program MOSREF. A detailed description of the program together with source program listings and sample outputs will be published separately (Tennant *et al* 1992b). Copies of this report are available from

the author. In each of the options below simulation or parameter refinement is for a site of any (known) symmetry in a crystal of any (known) symmetry.

(a) Single resonant site; nuclear electric quadrupole interaction only; no Goldanskii–Karyagan Effect (GKE).

(b) Single resonant site; combined nuclear electric quadrupole and magnetic field interactions; no GKE.

(c) As in (a) but including GKE; single or multiple resonant sites.

(d) As in (b) but including GKE; single or multiple resonant sites.

In options (b) and (d) there can be either or both external and internal magnetic fields. It is assumed that at least the orientation or an external field is known in parameter refinement options.

References

Aldridge L P, Finch J, Gainsford J, Patterson K H and Tennant W C 1991 *Phys. Chem. Miner.* **17** 583–90

Blume M and Kistner O C 1968 *Phys. Rev.* **171** 417–25

Boolchand P, Pradhan S, Wu Y, Abdelgadir M, Huff W, Farrell D, Coussement R and McDaniel D 1992 *Phys. Rev.* B **45** 921–30

Clark M G, Bancroft G M and Stone A J 1967 *J. Chem. Phys.* **47** 4250–61

Gibb T C 1974 *J. Phys. C: Solid State Phys.* **7** 1001–14

—— 1978 *J. Chem. Soc., Dalton Trans.* 743–52

Grant R W, Housley R M and Gonser U 1969 *Phys. Rev.* **178** 523–30

Housley R M, Grant R W and Gonser U 1969 *Phys. Rev.* **178** 514–22

McGavin D G, Palmer R A, Singers W A and Tennant W C 1980 *J. Magn. Reson.* **40** 69–81

McGavin D G and Tennant W C 1985 *Mol. Phys.* **55** 853–66

Mombourquette M J, Tennant W C and Weil J A 1986 *J. Chem. Phys.* **85** 68–79

Morè J J, Garbow B S and Hillstrom K E 1980 User Guide for MINPACK-1 *Argonne National Laboratory Publication* ANL-80-74

Nye J F 1957 *Physical Properties of Crystals, Their Representation by Tensors and Matrices* (Oxford: Clarendon)

Rae A D 1969 *J. Chem. Phys.* **50** 2672–85

Tennant W C, Finch J, Aldridge L P and Gainsford G J 1992a *J. Phys.: Condens. Matter* **4** 5447–59

Tennant W C, McGavin D G and Patterson K H 1992b *New Zealand Department of Science and Industrial Research Report No* CD 2425

Weil J A, Buch T and Clapp J E 1973 *Adv. Magn. Reson.* **6** 183–257

Zimmermann R 1975 *Nucl. Instrum. Methods* **128** 537–43

—— 1983 *Advances in Mössbauer Spectroscopy* ed B V Thosar, J K Srivastava, P K Iyengar and S C Bhargava (Amsterdam: Elsevier) pp 273–315

Zory P 1965 *Phys. Rev.* **140** A1401–07